Anisotropic transport properties of the two-dimensional electron gas in ordered-disordered $GaInP_2$ homojunctions: The structure of ordered domains

F. A. J. M. Driessen, G. J. Bauhuis, P. R. Hageman, A. van Geelen, and L. J. Giling
Department of Experimental Solid State Physics, Research Institute for Materials, University of Nijmegen, Toernooiveld, NL 6525 ED Nijmegen, The Netherlands
(Received 20 June 1994; revised manuscript received 29 August 1994)

The modulation-doped ordered-$GaInP_2$/disordered-$GaInP_2$ homojunction is presented. Capacitance-voltage (CV) profiling techniques, temperature-dependent Hall and resistivity measurements, cross-sectional transverse electron micrographs (TEM), and high-field magnetotransport have been used to characterize this structure grown by metal-organic vapor-phase epitaxy. The CV measurements showed a narrow profile at the homointerface with an order of magnitude reduction in carrier density within 3 nm. Typical two-dimensional behavior was observed from Hall data showing sheet carrier densities as high as 3.6×10^{13} cm^{-2} without carrier freeze-out, and constant mobilities around 900 $cm^2V^{-1}s^{-1}$ below $T=100$ K. The 300-K channel conductivity of this junction is 3.2×10^{-3} Ω^{-1}, which is higher than reported for other two-dimensional electron gases. By proper choice of the substrate orientation, domains of only the $(11\bar{1})$ ordering variant were present. TEM showed elongated shapes of average thickness 3.5–6 nm and length 75 nm in the (011) plane. By using Hall bars with different current directions, an asymmetry is observed for the contributions to the scattering mechanisms which determine the mobility: "mesoscopic" interface-roughness scattering for $T<100$ K and cluster scattering for $100<T<300$ K. Polar optical scattering at $T>300$ K indicates strong electron-phonon coupling. This asymmetry shows that the domain length in the (011) plane is larger than that in the $(01\bar{1})$ plane. The magnetoresistance ρ_{xx} and the Hall resistance ρ_{xy} show oscillations in reciprocal magnetic field involving an excited subband i with $n_{2D}^{i}=7.6\times10^{11}$ cm^{-2}, where 2D denotes two dimensional. The ρ_{xy} versus B curve shows features of a slight parallel conduction.

I. INTRODUCTION

The alloy $Ga_{0.52}In_{0.48}P$ (hereafter referred to as $GaInP_2$) is of technological importance because it is lattice matched to GaAs, has a high band gap (~1.9 eV at room temperature), and exhibits additional favorable properties, such as the absence of deep donor (DX) centers.[1] Depending on the conditions of growth, $GaInP_2$ forms either a random alloy (disordered state) or shows monolayer superlattice ordering in the $\langle 111\rangle$ directions (CuPt-type ordering). This ordered state has a reduced band gap owing to the level repulsion between different symmetry states of the binary constituents. This reduction is predicted to be as high as 260 meV if the alloy is entirely ordered.[2] However, in practice, only partial ordering into platelike domains occurs, and only two out of the four $\langle 111\rangle$ ordering variants appear. This type of ordering was initially unexpected because total-energy calculations indicated that bulk materials with ordering on the $\{100\}$ and $\{210\}$ planes are thermodynamically more stable.[3,4] Froyen and Zunger[5] showed that the ordering mechanism can be explained by surface thermodynamics: it also appears to involve surface reconstruction, the diffusion of atoms to the surface, and the attachment of adatoms at steps and kinks.[6] Anomalous properties, predominantly at low temperature, have been reported for ordered $GaInP_2$, caused by spatial separation of carriers[7,8] combined with the presence of quasi-two-dimensional residual donors.[9,10] For electronic applications, the two band-gap states of $GaInP_2$ offer challenging opportunities because band-gap engineering is possible only by changing the conditions of growth. The number of nonradiative interface states is expected to be lower than that of heterointerfaces because, first, there is no change in materials or composition at the interface and, second, the ordered and the disordered layers can be grown strain-free. This should improve the electrical quality of the interface, as has indeed been observed recently.[11]

In this paper, the first modulation-doped *o*(ordered)-$GaInP_2$/*d*(disordered)-$GaInP_2$ homojunction is presented along with a detailed investigation of its structural and electrical properties. Besides very good two-dimensional (2D) properties, it will be shown that this system enables us to obtain new structural information on the ordered domains. The optical properties of this sample will be the subject of a forthcoming publication.[12]

II. EXPERIMENTAL DETAILS

The sample was grown by metal-organic vapor-phase epitaxy at a pressure of 20 mbar with AsH_3, PH_3, trimethylgallium, and "solution-trimethylindium"[13] as precursors. The structure was grown on a (100) 6° off towards $[11\bar{1}]$, semi-insulating GaAs substrate, and consisted sequentially of a 0.3-μm undoped GaAs buffer layer, a 0.5-μm long-range-ordered undoped $GaInP_2$ layer (low band gap), and a disordered-$GaInP_2$ layer (high band gap), in which a 5-nm undoped spacer layer was followed

by a 100 nm uniformly n-doped layer with $n=4\times10^{18}$ cm^{-3}. The background concentration in the undoped layers was $n=6\times10^{14}$ cm^{-3}. Switching between the o and the d state was achieved by simultaneously increasing the growth temperature from 640 to 720 °C and decreasing the V-III ratio from 400 to 125 during a growth interruption. We selected only the $(11\bar{1})$ ordering variant by using the aforementioned substrate.[14,15] Ohmic Ni/AuGe/Ni contacts were evaporated on the samples prior to photolithographic etching into Hall bars. We processed three Hall bars, which were oriented in the $[01\bar{1}]$, [010], and [011] directions.

Cross-sectional transverse electron microscope (TEM) and high-resolution TEM measurements were performed on an ordered epilayer grown on the aforementioned substrate at the Delft Centre for Electron Microscopy. Capacitance-voltage (CV) measurements were performed in depletion mode at $T=300$ K using a Polaron profiler. Hall and resistivity measurements were performed on the bar-shaped samples in a flow cryostat with temperature tuning between 10 and 450 K; at higher temperatures, intrinsic conduction through the GaAs substrate influenced the measurements. The magnetic field in these experiments was 0.6 T. The diagonal (ρ_{xx}) and off-diagonal (ρ_{xy}) components of the resistivity tensor were measured in a 20-T Bitter magnet in the High-Field Magnet Laboratory (Nijmegen).

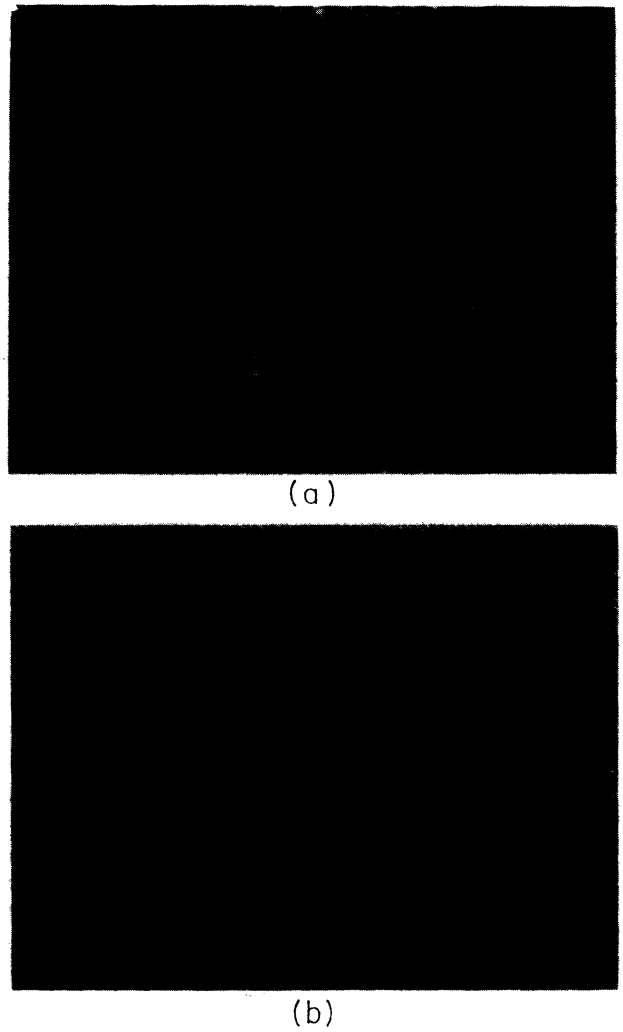

FIG. 1. (a) Dark-field micrographs formed using ordering reflections. (b) High-resolution TEM image of the (011) plane.

III. RESULTS AND DISCUSSION

The morphology of the ordered microstructure is difficult to describe, both because of the simultaneous existence of important structural features of very different sizes and because of the way these features interlock. The low-magnification, dark-field TEM image of an ordered epilayer grown on a (100) 6° towards $[11\bar{1}]$ substrate at $T_g=640$ °C is shown in Fig. 1(a). A platelike morphology is observed where the plates are inclined at an angle of 24° to the substrate; these plates correspond to the ordered regions.

Figure 1(b) shows a high-resolution TEM image. Large platelike $(GaP)_1(InP)_1$ domains are observed with fringes with a periodicity of 0.647 nm, which is virtually the double lattice constant of $GaInP_2$ in the $[11\bar{1}]$ direction. These domains are separated either by antiphase boundaries or by disordered $GaInP_2$, the fringe spacing of which is half that of the superlattice. The antiphase boundaries are observed through 180° phase shifts of the fringe pattern. From Fig. 1(b) and images of lower magnification, the average size of the ordered domains can be estimated to be between 3.5 and 6 nm for the plate thickness and >75 nm for the plate length in the (011) plane. No information of the size along the [011] direction can be obtained because only ordering reflections are observed at (011) and not at $(01\bar{1})$ cross sections. Therefore, orthorhombic shapes of the domains are assumed. It will be shown in this paper that the average domain length in the $(01\bar{1})$ plane is significantly smaller than that in the (011) plane. The situation is elucidated in Fig. 2(a).

A schematic of the anisotropic sample and the charge distribution in it is given in Fig. 2(b). For inhomogeneous media like the (partially) o-$GaInP_2$ state, it is difficult to

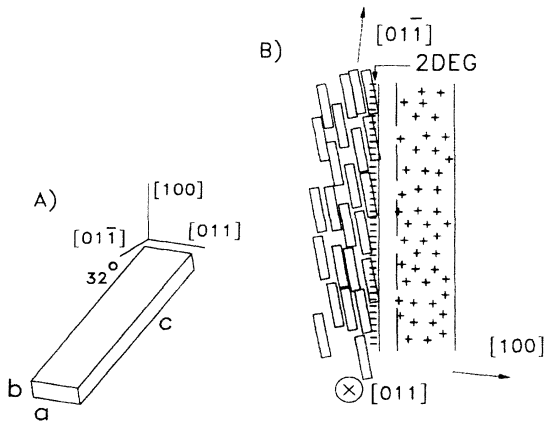

FIG. 2. (a) Orientation of the ordered domains; [100] is the direction of growth. Average values for b and c are 3.5–6 nm and >75 nm. (b) Schematic of the samples and the charge distribution in it; at the left is the "ordered state."

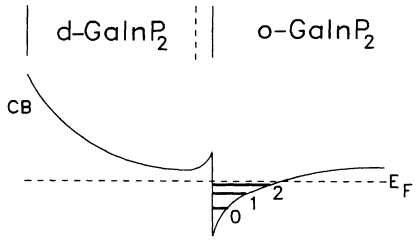

FIG. 3. Conduction-band structure of the *o-d* $GaInP_2$ modulation-doped homojunction.

maintain the concept of a band structure. However, the onset of signal recorded with photoluminescence excitation spectroscopy[16] is fairly sharp for partially ordered samples and can be used as a measure of the band gap.[17] The conduction band structure of the modulation-doped junction is shown in Fig. 3.

To probe the presence of a two-dimensional electron gas (2DEG) we used CV profiling. Although the classical theory for CV measurements does not apply strictly to the 2D quantum-mechanical system, the technique has proved valuable for these degenerate systems.[18] In modulation-doped heterostructures with no detectable parallel conductance, the depletion of the 2DEG during CV profiling begins already at zero-bias voltage, as can be seen for our sample in Fig. 4. The profile shows a high carrier density at the *d*-$GaInP_2$/*o*-$GaInP_2$ interface, which decreases by one order of magnitude within 3 nm from the interface. Because of majority-carrier diffusion, this depth is an upper limit.[19] The strong spatial localization of the 2DEG is unambiguously shown here.

Figure 5 shows the temperature dependence of the sheet carrier density n_{2D} as measured with the Hall technique for the various current directions. No freeze-out of

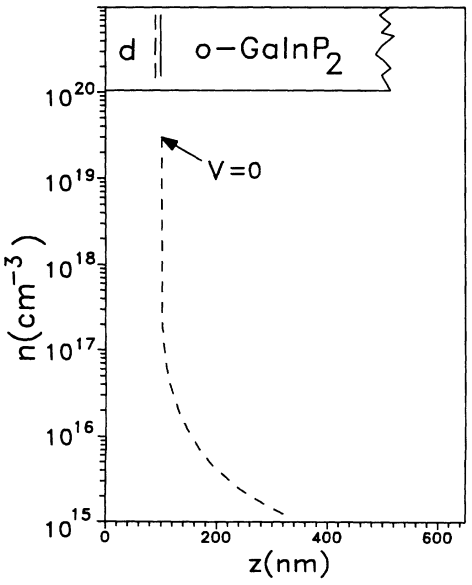

FIG. 4. Capacitance-voltage profile recorded at $T=300$ K; the inset shows the sample structure.

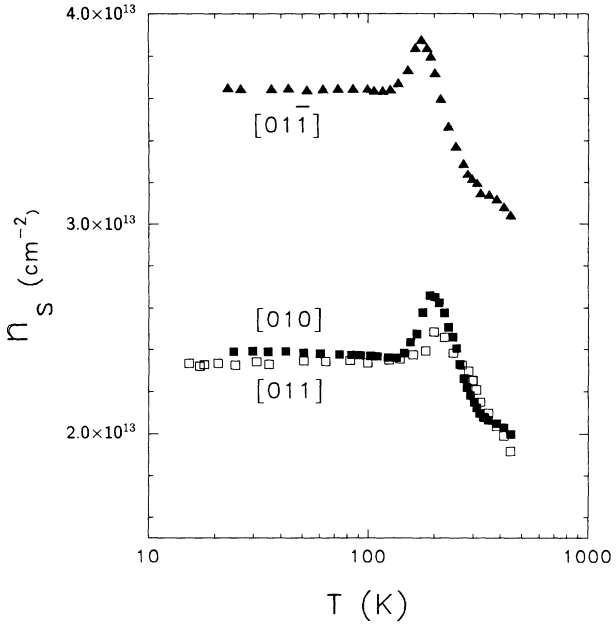

FIG. 5. Sheet carrier density vs temperature. The current directions were parallel to [01$\bar{1}$], [010], and [011] for the upper, middle, and lower graph, respectively.

carriers is observed below $T=100$ K, which confirms the formation of a 2DEG. The n_{2D} was 2.4×10^{13} cm^{-2} for the samples with bars in the [010] and [011] directions and 3.6×10^{13} cm^{-2} for that in the [01$\bar{1}$] direction. The latter higher value results from a lateral inhomogeneity across the wafer.[20] With increasing temperature the carrier concentration first increases, as has been observed earlier in 2D systems,[21] but then shows an unprecedented decrease. This decrease is not dramatic (an n_{2D} of 2.0×10^{13} cm^{-2} remains at room temperature) and is most probably caused by delocalization[9,10] of a fraction of the carriers out of the ordered domains, so that the conductive layer broadens slightly. It should be borne in mind that the 2DEG is still strongly confined at the interface at 300 K because the CV profile was taken at this temperature. To our knowledge, the above sheet carrier densities are the highest reported in any III/V heterostructure; this includes δ-doped samples, which are especially known for their high n_{2D}.[22] We infer a combination of reasons for this: the absence of carrier-trapping DX centers in $GaInP_2$; the previously mentioned reduction in nonradiative interface states owing to the homoepitaxy; and finally, the absence of Al in the sample, which reacts very quickly with residual traces of oxygen and water during growth, and thereby forms deep centers.[23]

For 2DEG's that are confined within an alloy, such as $In_{0.53}Ga_{0.47}As/Al_{0.52}In_{0.48}As$, alloy-disorder (AL) scattering is usually the primary scattering mechanism limiting the mobility at low temperature.[24,25] This μ_{AL} is virtually independent of temperature. As will be shown in the Appendix, mobilities in the range 2600–7000 cm^2/Vs would then be expected for the *o-d* $GaInP_2$ 2DEG. Figure 6 shows the Hall mobility μ_H as a function of temperature

for the cases where the drain-to-source contacts of the Hall bars were directed in the [01$\bar{1}$], [010], and [011] directions. All curves show a constant mobility below $T \approx 100$ K, which is consistent with the temperature behavior of AL scattering. However, all curves show a significantly lower mobility than the above estimate for μ_{AL}. Occupation of more than two subbands will reduce this estimate only slightly. Therefore, it is concluded that another scattering mechanism dominates here. It will be shown below that this is interface roughness (IFR) scattering. This IFR scattering is generally neglected in calculations for modulation-doped 2D systems in III-V materials because of atomic flatness of the interfaces, but it cannot be neglected in the inhomogeneous ordered layer.

Below $T = 100$ K, the μ_H for the [011] direction is just one-half that for the [01$\bar{1}$] direction; for the [010] direction the value is intermediate. From Ref. 9 we know that electrons are confined in the ordered domains at these temperatures. Therefore, electrons move across the whole length c of an ordered platelike domain for the [01$\bar{1}$] direction before they tunnel to a neighboring domain, whereas for the [011] direction electrons traverse the distances between adjacent domains a. Because the mobility is lower for the [011] direction, this suggests a larger number of tunneling events as compared with the [01$\bar{1}$] direction. This means that either $\bar{a} < \bar{c}$ and/or that the distances between the domains are larger for the [011] direction. In fact, this behavior is an example of IFR scattering in quantum wells[26] in the limit that the change in well width $\Delta(\mathbf{r})$ equals the well width L_z ($=b$ in Fig. 2). The mobility μ_{IFR} limited by IFR scattering is then given by

$$\mu_{IFR} \propto \frac{b^4}{\Lambda^2} g(n_{2D}, T, \Lambda) , \tag{1}$$

where Λ is the lateral size of the Gaussian fluctuations of the interface: For our system, Λ is the mean distance between ordered domains with $\Lambda[011] \neq \Lambda[01\bar{1}]$. The function $g(n_{2D}, T, \Lambda)$ is given in Ref. 27 and is particularly sensitive towards variations of Λ; its value is minimal if $\Lambda = 2/q \sim \pi/2k_F$, where k_F is the Fermi wave vector. Therefore, μ_{IFR} depends strongly on variations of the Fermi vectors of the various subbands, and therefore on their occupancy. Optimization of these parameters, therefore, provides a tool for improvement of the low-temperature mobility. Our measured values of the mobility lie in the same range as those of μ_{IFR} for quantum wells of similar thickness (4 nm). The limiting scattering mechanism can therefore be described as a mesoscopic variant of IFR scattering.

The measured temperature behavior of mobility is also consistent with that of μ_{IFR}. While $g(T)$ is constant below 100 K, above this temperature it increases and therefore μ_{IFR} does not limit the mobility any longer. At higher temperatures, electrons start to become delocalized and scatter at ordered clusters. This cluster scattering can be calculated using the Harrison-Hauser/Marsh formalism;[28] it was indeed observed in ordered $GaInP_2$.[10] The typical "U-shaped" behavior of the cluster Hall mobility μ_H^{CL} for intermediate values of cluster radius r_c (Ref. 29) is observed in the upper graph in Fig. 6 between $T = 120$ and 300 K. Similar behavior is observed for the [010] direction, however, the maximum value of μ_H has shifted to higher temperature, which corresponds to an enhanced cross section for cluster scattering. The lower graph of Fig. 6 shows the largest effect of cluster scattering: it even dominates at 450 K and the minimum in the "U curve" has smoothed out. This proves that the cross section for cluster scattering is smaller for the [01$\bar{1}$] current direction than for the [011] direction, which implies that $\bar{a} < \bar{c}$, as is shown in Fig. 2(a).

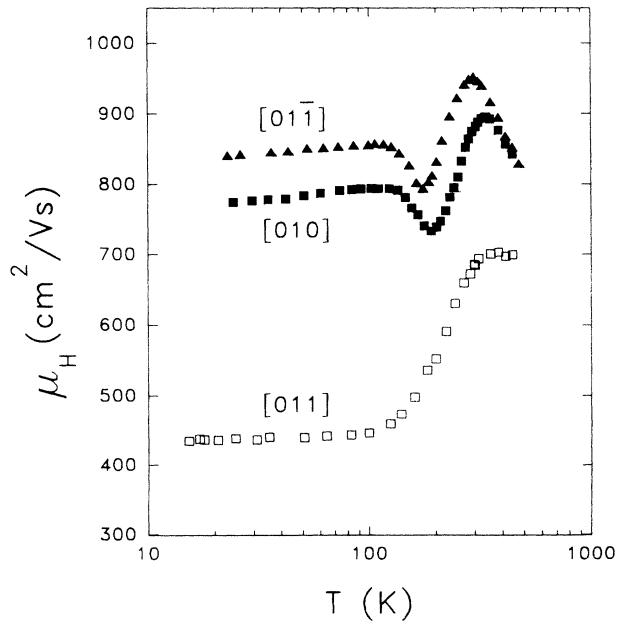

FIG. 6. Mobility vs temperature. The current directions were parallel to [01$\bar{1}$], [010], and [011] for the upper, middle, and lower graph, respectively.

Finally, we turn to the temperature regime above 300 K. Figure 6 shows that at such temperatures the mobility is limited by an angular-independent scattering mechanism, because the [011] and [010] curves approach one another, as would the [01$\bar{1}$] curve at higher temperature. The temperature behavior suggests polar-optical-phonon (PO) scattering for which $\mu_{PO} \propto T^{-\beta}$ with $\beta \geq 2$. There exist different approaches to calculate this scattering mechanism in two dimensions. Hirakawa and Sasaki[30] used a 2D variant in their calculations. Because of electron-phonon interaction, μ_{PO} is then proportional to $n_{2D}^{-1/3}$. Such behavior has been observed in Si–metal-oxide-semiconductor inversion layers but not in $GaAs/Al_xGa_{1-x}As$ and $In_{0.53}Ga_{0.47}As/Al_{0.52}In_{0.48}As$ 2DEG's. Walukiewicz *et al.*[24] argued that a three-dimensional approach could be used for the III-V cases. With the 3D variant we find $\mu_{PO} \cong 3000$ cm^2/Vs at 450 K (see Ref. 10); for the 2D variant $\mu_{PO} = AT^{-2}n_{2D}^{-1/3}$, with $A \cong 5.5 \times 10^7$ cm^3/Vs (as deduced from Fig. 4 in Ref. 30). At 450 K, the latter equation yields $\mu_{PO} \cong 7 \times 10^2$ cm^2/Vs, which shows reasonably good agreement with our data. This suggests that the 2D variant is valid for the $GaInP_2$

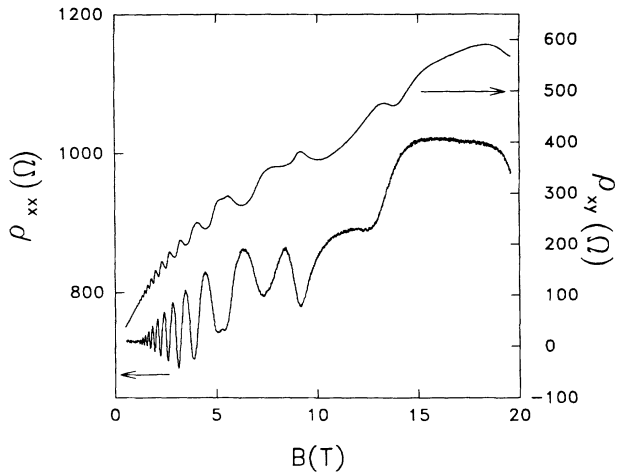

FIG. 7. Magnetoresistance ρ_{xx} and Hall resistance ρ_{xy} vs magnetic field at $T=4.2$ K; the current direction was parallel to $[01\bar{1}]$.

2DEG system, which implies the presence of strong electron-phonon coupling.

Figure 7 shows Shubnikov–de Haas (SdH) data (lower trace). At low fields the minima in the magneto-oscillations decrease monotonically. This periodicity in reciprocal field corresponds to a sheet carrier concentration of 7.6×10^{11} cm^{2}V^{-1}s^{-1}. Above $B=4$ T, interference from a second periodicity occurs whereupon the minima in SdH oscillations are seen to increase again. This rise may also be caused by a slight parallel conduction. The Hall resistance ρ_{xy} as a function of B is shown in the upper trace of Fig. 7. Concomitant with the minima in ρ_{xx}, ρ_{xy} shows deviations from linear behavior; a weak quantum Hall effect. The slope of the ρ_{xy} versus B curve at low fields yields the previously mentioned total sheet carrier density of 3.6×10^{13} cm^{-2}. The Hall resistance is sublinear in B, which points to a slight parallel conduction.[31,32] The periodic behavior of ρ_{xx} and ρ_{xy} with its "low" sheet carrier concentration is attributed to a populated higher subband. Oscillatory behavior from the lowest subband E_0 is not yet observed because the width of its Landau levels is larger than the splitting between these levels at the fields available.

For high-speed operation of electronic devices, the 2D channel conductivity ($\sigma_{ch}=en_{2D}\mu$) at room temperature must be maximized. In Table I the σ_{ch} for this $GaInP_2$ 2DEG (the $[01\bar{1}]$ data) is compared with that of 2DEG's in $GaAs/Al_xGa_{1-x}As$, $In_{0.53}Ga_{0.47}As/Al_{0.52}In_{0.48}As$, and δ field-effect transistors (FET's) both at temperatures of 4.2 and 300 K. Despite its lower value at 4.2 K, the σ_{ch} of *o-d* $GaInP_2$ surpasses those of the others at 300 K. This remarkably high value is caused by the temperature dependence of the mobility and makes the *o-d* $GaInP_2$ 2DEG suitable for application in electronic devices. A further increase in σ_{ch} can be expected if spacer thicknesses of ~30 nm are used,[24] and if the ordered domains are enlarged, as can be expected at lower growth rates.[33]

TABLE I. Channel conductivities at $T=4$ and 300 K for various two-dimensional electron gases.

	$\sigma_{ch}^{4\,K}$ (Ω^{-1})	$\sigma_{ch}^{300\,K}$ (Ω^{-1})
o-d $GaInP_2$	5.0×10^{-3}	3.2×10^{-3}
$GaAs/Al_xGa_{1-x}As$[a]	1.1×10^{-1}	1.1×10^{-3}
$In_{0.53}Ga_{0.47}As/Al_{0.52}In_{0.48}As$[b]	9.4×10^{-3}	9.4×10^{-4}
δ FET[c]	1.3×10^{-3}	9.6×10^{-4}

[a]From Ref. 24.
[b]From Ref. 34.
[c]From Ref. 22.

IV. CONCLUSIONS

We have prepared and characterized the first two-dimensional electron gas in modulation-doped *o*-$GaInP_2$/*d*-$GaInP_2$ homojunctions. High-resolution TEM images show a high degree of ordering. Temperature-dependent Hall and resistivity measurements revealed 2D behavior with an extremely high sheet carrier concentration of $n_{2D}=3.6\times10^{13}$ cm^{-2} and constant mobility around 900 cm^{2}V^{-1}s^{-1} below $T=100$ K. A sharp CV profile at the *o-d* interface confirmed the dense 2DEG. The system exhibits the highest channel conductivity at $T=300$ K reported so far and is therefore suited for the fabrication of high-speed electronic devices. The effect of various scattering mechanisms on the mobility was investigated. The dominant scattering mechanisms are mesoscopic interface roughness scattering for $T<100$ K, cluster scattering for $100<T<300$ K, and polar-optical-phonon scattering for $T>300$ K, with an indication for strong electron-phonon coupling. Transport phenomena were used to probe the structure of the ordered domains, yielding information on the previously unknown domain length in the $(01\bar{1})$ plane. Finally, periodic oscillations in reciprocal magnetic field were observed for ρ_{xx} and ρ_{xy}. They originate from an excited subband i with $n_{2D}^i=7.6\times10^{11}$ cm^{-2}.[34]

ACKNOWLEDGMENTS

Financial support from the Stichting voor Fundamenteel Onderzoek der Materie (FOM) and the Nederlandse Organisatie voor Energie en Milieu (NOVEM) is gratefully acknowledged, as is D. M. Frigo for critically reading the manuscript.

APPENDIX

As a result of the high n_{2D} in the $GaInP_2$ junction, at least two subbands are occupied. Therefore, apart from intrasubband scattering, these subbands must be treated in general as coupled through intersubband scattering. The major effect of an unoccupied subband is that it provides final states available for the scattering of electrons. For two occupied subbands no such scattering is possible, which leads to a reduction of the electron mobility. If two occupied subbands are assumed, the following relationship holds for the relaxation time τ_{AL}:

TABLE II. Summary of the parameters used to calculate μ_{AL} for $GaInP_2$.

	$In_{0.53}Ga_{0.47}As/Al_{0.52}In_{0.48}As$	*o-d* $GaInP_2$
m^* (units of m)	0.05	0.105
Ω (nm^3)	0.587[3]	0.565[3]
V	0.6	$\sim 0.6-1$[a]
n_{2D} (cm^{-2})	6.5×10^{11}	3.5×10^{13}
μ_{AL} (cm^2/Vs)	1.2×10^5	

[a]This alloy-disorder scattering parameter V is of order 1 but is not known precisely; we assume it to lie between 0.6 and 1, the values for $In_{0.53}Ga_{0.47}As/Al_{0.52}In_{0.48}As$ and $GaAs/Al_xGa_{1-x}As$ (Ref. 24).

$$\frac{1}{\tau_{AL}}=\frac{m^*x(1-x)\Omega\langle V\rangle^2}{\hbar^3}\left[\sum_{i=0}^{1} I^i_{AL}+\sum_{i,j=0;j>i}^{2} I^{i,j}_{AL}\right], \tag{A1}$$

where m^* is the effective mass in units of the free-electron mass, x is the fraction of the alloy, Ω the volume of the unit cell, V the alloy-disorder scattering parameter, and I^i_{AL} and $I^{i,j}_{AL}$ are integrals reflecting intrasubband and intersubband scattering, respectively (see Ref. 24). The sum of the integrals can be shown to be proportional to $(n'_{2D})^{0.36}=(n_{2D}+n_{depl})^{0.36}$ with $n_{depl}(cm^{-2})$ the background concentration of charge in the depleted region. To estimate the μ_{AL} of the $GaInP_2$ 2DEG we compare it with a system in which the 2DEG is also confined in the alloy: the $In_{0.53}Ga_{0.47}As/Al_{0.52}In_{0.48}As$ modulation-doped heterojunction with two occupied subbands.[24] From Eq. (A1) and the insensitivity of τ_{AL} on energy, it follows that

$$\frac{\mu_{AL-2}}{\mu_{AL-1}}=\left[\frac{m^*_1}{m^*_2}\right]^2\frac{\Omega_1}{\Omega_2}\left[\frac{\langle V\rangle_1}{\langle V\rangle_2}\right]^2\left[\frac{n'_1}{n'_2}\right]^{0.36}_{2D}, \tag{A2}$$

where the subscripts 1 and 2 refer to $In_xGa_{1-x}As$ and $Ga_{1-x}In_xP$, respectively. Inserting the parameters summarized in Table II for $GaInP_2$ yields $\mu_{AL-2}\approx 2600-7000\ cm^2/Vs$ for $V_2\in(0.6,1)$.

[1]D. Costa and J. Harris, Jr., IEEE Trans. Electron Devices **ED-59**, 2383 (1992).

[2]S.-H. Wei and A. Zunger, Appl. Phys. Lett. **56**, 662 (1990).

[3]J. E. Dandrea, L. G. Ferreira, S. Froyen, S.-H. Wei, and A. Zunger, Appl. Phys. Lett. **56**, 731 (1990).

[4]G. P. Srivastava, J. L. Martins, and A. Zunger, Phys. Rev. B **31**, 2561 (1985).

[5]S. Froyen and A. Zunger, Phys. Rev. Lett. **66**, 2132 (1991).

[6]G. S. Chen and G. B. Stringfellow, *Proceedings of the 19th International Symposium on Gallium Arsenide and Related Compounds* (Institute of Physics, Bristol, 1992).

[7]J. E. Fouquet, V. M. Robbins, J. Rosner, and O. Blum, Appl. Phys. Lett. **57**, 1566 (1990).

[8]M. C. DeLong, W. D. Ohlsen, I. Viohl, P. C. Taylor, and J. M. Olson, J. Appl. Phys. **70**, 2780 (1991).

[9]F. A. J. M. Driessen, G. J. Bauhuis, S. M. Olsthoorn, and L. J. Giling, Phys. Rev. B **48**, 7889 (1993).

[10]G. J. Bauhuis, F. A. J. M. Driessen, and L. J. Giling, Phys. Rev. B **48**, 17 239 (1993).

[11]R. A. J. Thomeer, A. van Geelen, and L. J. Giling (unpublished).

[12]F. A. J. M. Driessen, P. R. Hageman, G. J. Bauhuis, S. M. Olsthoorn, and L. J. Giling (unpublished).

[13]D. M. Frigo, W. W. van Berkel, W. A. H. Maassen, G. P. M. van Mier, J. H. Wilkie, and A. W. Gal, J. Cryst. Growth **124**, 99 (1992).

[14]P. Bellon, J. P. Chevalier, E. Augard, J. P. André, and G. P. Martin, J. Appl. Phys. **66**, 2388 (1989).

[15]A. Gomyo, S. Kawata, T. Suzuki, S. Iijima, and I. Hino, Jpn. J. Appl. Phys. **10**, L1728 (1989).

[16]M. C. DeLong, D. J. Mowbray, R. A. Hogg, M. S. Skolnick, M. Hopkinson, J. P. R. David, P. C. Taylor, S. R. Kurtz, and J. M. Olson, J. Appl. Phys. **73**, 5163 (1993).

[17]The photon energy of the PL signal is no measure of the band gap because it strongly depends on impurities, depletion fields, and band-filling effects.

[18]E. F. Schubert, K. Ploog, H. Dämbkes, and K. Heime, Appl. Phys. A **33**, 63 (1984).

[19]D. V. Lang, R. A. Logan, and M. Jaros, Phys. Rev. B **19**, 1015 (1979).

[20]The reason for this difference is that our initial $[01\bar{1}]$ sample, with an $n_{2D}=2.0\times10^{13}\ cm^{-2}$ at T_{room}, broke during cooling. Hence, a new $[01\bar{1}]$ bar had to be processed from a different part of the 2-in. wafer. The increase in n_{2D} for the $[01\bar{1}]$ direction, therefore, results from a lateral inhomogeneity across the wafer.

[21]R. Dingle, H. Störmer, A. Gossard, and W. Wiegmann, Appl. Phys. Lett. **33**, 665 (1978).

[22]N. Pan, J. Carter, G. S. Jackson, H. Hendriks, J. C. Huang, and X. L. Zheng, *Proceedings of the 17th International Symposium on Gallium Arsenide and Related Compounds* (Institute of Physics, Bristol, 1990).

[23]J. Zhang, B. M. Keyes, S. E. Asher, R. K. Ahrenkiel, and M. L. Timmons, Appl. Phys. Lett. **63**, 1369 (1993).

[24]W. Walukiewicz, H. E. Ruda, J. Logowski, and H. C. Gatos, Phys. Rev. B **30**, 4571 (1984).

[25]An estimate for the mobility caused by remote ionized impurity scattering, which increases according to $n_{2D}^{1.4}$, yields at $n_{2D}=3.5\times10^{13}\ cm^{-2}$ and spacer thickness of 5 nm: $\mu_{RI}\simeq(0.5-1.0)\times10^6\ cm^2/Vs$. This is orders of magnitude larger than μ_{AL} and can, therefore, be neglected. The contribution of other scattering mechanisms is even lower.

[26]H. Sasaki, T. Noda, K. Hirakawa, M. Tanaka, and T. Matsusue, Appl. Phys. Lett. **51**, 1934 (1987).

[27]A. Gold and V. T. Dolgopolov, Phys. Rev. B **33**, 1076 (1986).

[28]J. H. Marsh, Appl. Phys. Lett. **41**, 732 (1982); J. W. Harrison and J. R. Hauser, Phys. Rev. B **13**, 5347 (1976); J. Appl. Phys. **47**, 292 (1976).

[29]D. J. Friedman, A. E. Kibbler, and J. M. Olson, Appl. Phys. Lett. **59**, 2998 (1991).

[30]K. Hirakawa and H. Sasaki, Phys. Rev. B **33**, 8291 (1986).

[31]R. L. Petritz, Phys. Rev. **110**, 1254 (1958).

[32]R. D. Larrabee and W. R. Thurber, IEEE Trans. Electron Devices **ED-27**, 32 (1980).

[33]D. S. Cao, E. H. Reihlen, G. S. Chen, A. W. Kimball, and G. B. Stringfellow, J. Cryst. Growth **109**, 279 (1991).

[34]A. Kastalsky, R. Dingle, K. Y. Cheng, and A. Y. Cho, Appl. Phys. Lett. **41**, 274 (1982).

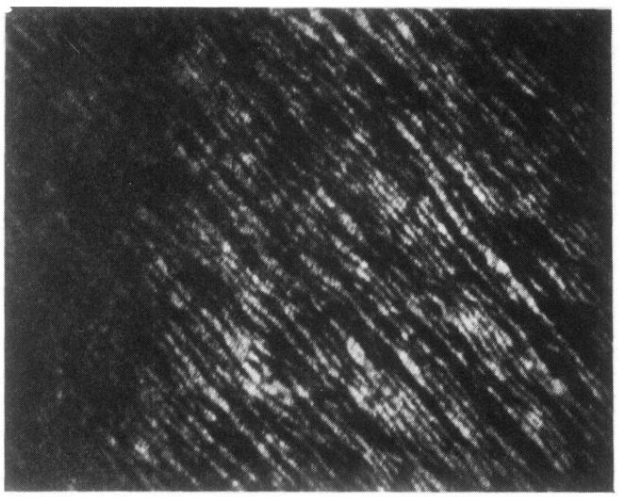

(a)

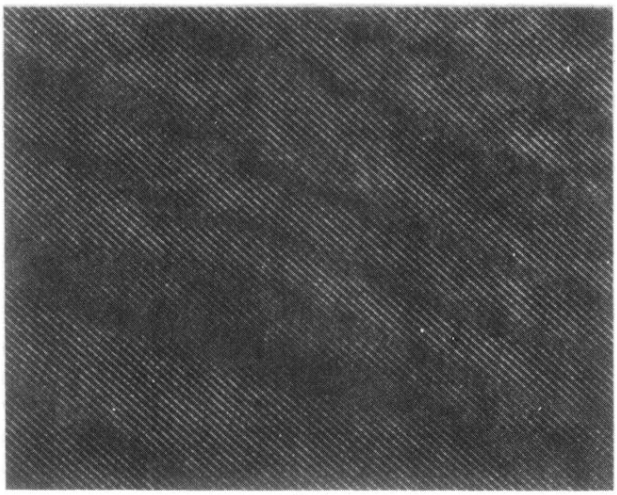

(b)

FIG. 1. (a) Dark-field micrographs formed using ordering reflections. (b) High-resolution TEM image of the (011) plane.